Article

Diabetes recovery by age-dependent conversion of pancreatic δ-cells into insulin producers

CHERA, Simona, *et al*.

Abstract

Total or near-total loss of insulin-producing β-cells occurs in type 1 diabetes. Restoration of insulin production in type 1 diabetes is thus a major medical challenge. We previously observed in mice in which β-cells are completely ablated that the pancreas reconstitutes new insulin-producing cells in the absence of autoimmunity. The process involves the contribution of islet non-β-cells; specifically, glucagon-producing α-cells begin producing insulin by a process of reprogramming (transdifferentiation) without proliferation. Here we show the influence of age on β-cell reconstitution from heterologous islet cells after near-total β-cell loss in mice. We found that senescence does not alter α-cell plasticity: α-cells can reprogram to produce insulin from puberty through to adulthood, and also in aged individuals, even a long time after β-cell loss. In contrast, before puberty there is no detectable α-cell conversion, although β-cell reconstitution after injury is more efficient, always leading to diabetes recovery. This process occurs through a newly discovered mechanism: the spontaneous en masse reprogramming [...]

Reference

CHERA, Simona, *et al*. Diabetes recovery by age-dependent conversion of pancreatic δ-cells into insulin producers. *Nature*, 2014, vol. 514, no. 7523, p. 503-7

DOI : 10.1038/nature13633
PMID : 25141178

LETTER

doi:10.1038/nature13633

Diabetes recovery by age-dependent conversion of pancreatic δ-cells into insulin producers

Simona Chera[1], Delphine Baronnier[1], Luiza Ghila[1], Valentina Cigliola[1], Jan N. Jensen[2], Guoqiang Gu[3], Kenichiro Furuyama[1], Fabrizio Thorel[1], Fiona M. Gribble[4], Frank Reimann[4] & Pedro L. Herrera[1]

Total or near-total loss of insulin-producing β-cells occurs in type 1 diabetes[1,2]. Restoration of insulin production in type 1 diabetes is thus a major medical challenge. We previously observed in mice in which β-cells are completely ablated that the pancreas reconstitutes new insulin-producing cells in the absence of autoimmunity[3]. The process involves the contribution of islet non-β-cells; specifically, glucagon-producing α-cells begin producing insulin by a process of reprogramming (transdifferentiation) without proliferation[3]. Here we show the influence of age on β-cell reconstitution from heterologous islet cells after near-total β-cell loss in mice. We found that senescence does not alter α-cell plasticity: α-cells can reprogram to produce insulin from puberty through to adulthood, and also in aged individuals, even a long time after β-cell loss. In contrast, before puberty there is no detectable α-cell conversion, although β-cell reconstitution after injury is more efficient, always leading to diabetes recovery. This process occurs through a newly discovered mechanism: the spontaneous *en masse* reprogramming of somatostatin-producing δ-cells. The juveniles display 'somatostatin-to-insulin' δ-cell conversion, involving dedifferentiation, proliferation and re-expression of islet developmental regulators. This juvenile adaptability relies, at least in part, upon the combined action of FoxO1 and downstream effectors. Restoration of insulin producing-cells from non-β-cell origins is thus enabled throughout life via δ- or α-cell spontaneous reprogramming. A landscape with multiple intra-islet cell interconversion events is emerging, offering new perspectives for therapy.

To determine how ageing affects the mode and efficiency of β-cell reconstitution after β-cell loss, we administered diphtheria toxin (DT) to adult (2-month-old) or aged (1- and 1.5-year-old) *RIP-DTR* mice, whose β-cells bear DT receptors[3], and followed them for up to 14 months. Collectively, we found that α-to-β-cell conversion is the main mechanism of insulin cell generation after massive β-cell loss in adult post-pubertal mice, whether middle-aged or very old, and that α-cells are progressively recruited into insulin production with time (Extended Data Fig. 1 and Supplementary Tables 1–5).

We focused on regeneration potential during early postnatal life by inducing β-cell ablation before weaning, at 2 weeks of age (Fig. 1a). We found that prepubescent mice rapidly recover from diabetes after near-total β-cell loss: 4 months later all mice were almost normoglycaemic, thus displaying a faster recovery relative to adults (Fig. 1b and Extended Data Fig. 2a, b; see also Extended Data Fig. 1a).

Histologically, 99% of β-cells were lost at 2 weeks after DT administration (Fig. 1c). The β-cell number increased by 45-fold 4 months after ablation, representing 23% of the normal age-matched β-cell mass (Fig. 1c and Supplementary Table 6) and correlating with recovery of normoglycaemia[1].

All animals remained normoglycaemic for the rest of their life (Supplementary Table 6). Mice were neither intolerant to glucose nor insulin resistant during the period of analysis, up to 15 months after injury (Extended Data Fig. 2c–e).

We investigated whether the new insulin$^+$ cells were reprogrammed α-cells, as in adults, using *glucagon-rtTA; TetO-Cre; R26-YFP; RIP-DTR* pups (Fig. 1d). We observed that almost no insulin$^+$ cells co-expressed yellow fluorescent protein (YFP) or glucagon (Supplementary Table 7), indicating that α-cells do not reprogram in juveniles.

We further explored the age-dependency of rescue after near-total β-cell loss. To this aim, normoglycaemic 5-month-old mice, which had recovered from β-cell loss at 2 weeks of age, were re-administered DT to ablate the regenerated insulin$^+$ cells. One month following the second ablation, 30% of the insulin-containing cells also contained glucagon (Extended Data Fig. 2f and Supplementary Table 8), like β-cell-ablated adults (Extended Data Fig. 1k), confirming that the pre-pubertal regeneration mechanism is restricted temporally.

We measured proliferation rates at different time-points over 2 months of regeneration. The proportion of Ki67-labelled insulin$^+$ cells was very low (Extended Data Fig. 2g and Supplementary Table 9), indicating that neither escaping β-cells nor regenerated insulin$^+$ cells proliferate during this period. However, there was a transient 3.5-fold increase in the number of insular Ki67$^+$ cells 2 weeks after ablation, unlike in adult animals (Extended Data Fig. 2h and Supplementary Table 10). Replicating cells were hormone-negative, chromogranin-A-negative, and were not lineage traced to either α- or escaping β-cells (Extended Data Fig. 2i, j).

Coincident with the peak of islet cell proliferation, we noticed in pups a 4.5-fold decrease in the number of somatostatin (Sst)-producing δ-cells (from 13 to 3 δ-cells per islet section; Extended Data Fig. 3a and Supplementary Table 11) and a 76-fold decrease of *Sst* transcripts (Extended Data Fig. 3b), without any indication of increased islet cell death. We therefore lineage traced δ-cells and observed that regenerated insulin-producing cells were dedifferentiated δ-cells. At 2 months of age in *Sst-Cre; R26-YFP; RIP-DTR* mice, about 81% of δ-cells were YFP$^+$ in the absence of β-cell ablation, whereas α- and β-cells were labelled at background levels (0.9% for β-cells and 0.2% for α-cells; Extended Data Fig. 3c, d and Supplementary Table 12). During β-cell reconstitution in pups, 2 weeks after β-cell ablation, 80% of YFP$^+$ cells were proliferating (Ki67$^+$) and Sst-negative (Fig. 2a, b and Supplementary Table 13), while most Ki67$^+$ cells were YFP-labelled (85%; Supplementary Table 14).

These observations suggest that in β-cell-ablated pre-pubertal mice most δ-cells undergo a loss of Sst expression and enter the cell cycle.

We further investigated the fate of proliferating dedifferentiated δ-cells. At 1.5 months post-ablation, most insulin$^+$ cells expressed YFP (90%), indicating their δ-cell origin (Fig. 2c, d and Supplementary Table 15). Furthermore, in contrast to non-ablated age-matched controls, where all YFP$^+$ cells were Sst$^+$ (>99%), about half of YFP$^+$ cells were insulin$^+$ after 1.5 months of regeneration (45%; Fig. 2e and Supplementary Table 16). This reveals that half of the progeny of dedifferentiated δ-cells becomes insulin expressers. Bihormonal Sst$^+$/insulin$^+$ cells were rare (Supplementary Table 17).

[1]Department of Genetic Medicine & Development, Faculty of Medicine, University of Geneva, 1 rue Michel-Servet, 1211 Geneva-4, Switzerland. [2]Novo Nordisk A/S, Niels Steensens Vej 6, DK-2820 Gentofte, Denmark. [3]Cell and Developmental Biology, Vanderbilt University Medical Center, 465 21st Av. South, Nashville, Tennessee 37232, USA. [4]Cambridge Institute for Medical Research, Hills Road, Cambridge CB2 0XY, UK.

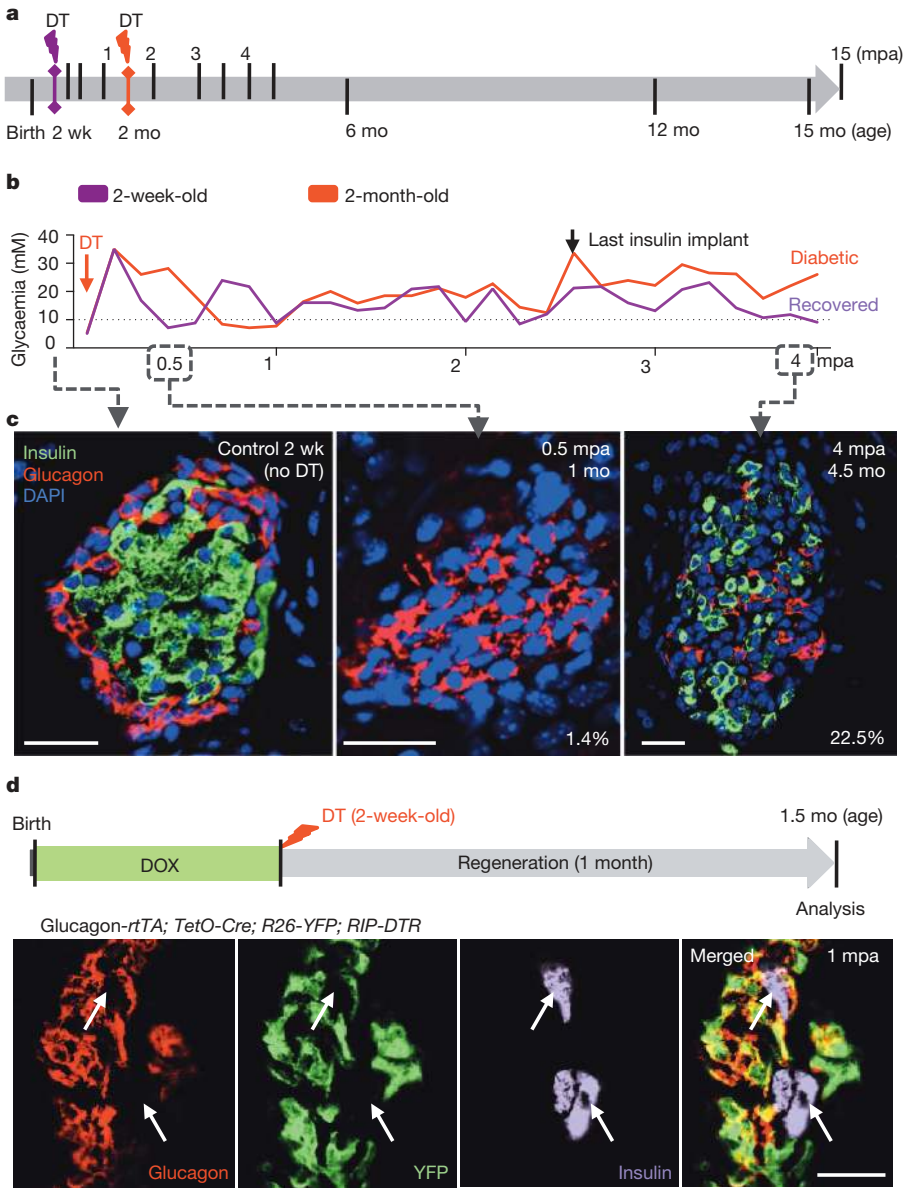

Figure 1 | β-cell ablation before puberty and diabetes recovery. **a**, Experimental designs depicting the ages at DT administration and the various analyses. mpa, months post-ablation. **b**, Comparative evolution of glycaemia in β-cell-ablated juveniles ($n = 5$) and middle-aged adults ($n = 4$); 2.5 months after β-cell ablation, insulin administration was stopped ($P = 0.0014$, Mann–Whitney test). Dotted line shows upper limit of normoglycaemia (10 mM). **c**, Islets from 2-week-old mice with no DT treatment (control), 1-month-old mice at 0.5 mpa and 4.5-month-old mice at 4 mpa (Supplementary Table 6). Percentages refer to β-cell mass relative to age-matched unablated controls. DAPI, 4′,6-diamidino-2-phenylindole. **d**, α-Cell tracing in pups. DOX, doxycycline. Scale bars, 20 μm.

Combined, these observations show that at the cell population level, each dedifferentiated δ-cell yields one insulin expresser cell and one Sst^+ cell (Extended Data Fig. 4).

We confirmed with two other assays that regeneration and diabetes recovery in juvenile mice are δ-cell-dependent: by inducing β-cell destruction with streptozotocin (STZ) instead of DT (Extended Data Fig. 5a–c), and by co-ablating β- and δ-cells simultaneously in *Sst-Cre; R26-YFP; R26-iDTR; RIP-DTR* pups. In the absence of δ-cells there was no $insulin^+$ cell regeneration, and no recovery (Fig. 2f).

In adults, δ-cells neither dedifferentiated nor proliferated after β-cell ablation (Extended Data Fig. 5d, e and Supplementary Table 20). Nevertheless, like α-cells, a few δ-cells reprogrammed into insulin production, so that after 1.5 month of regeneration 17% of the rare insulin-producing cells were YFP^+, that is, δ-cell-derived (Extended Data Fig. 5f–h and Supplementary Tables 21, 22).

By transplanting *Sst-Cre; R26-YFP; RIP-DTR* juvenile islets into adult wild-type mice we observed that, following β-cell ablation, the newly formed $insulin^+$ cells were reprogrammed δ-cells, thus showing that the pup-specific regeneration is intrinsic to islets (Extended Data Fig. 6).

Contrary to β-cells in age-matched adult mice, δ-cell-derived $insulin^+$ cells replicated transiently (Extended Data Fig. 7a and Supplementary Table 23); the β-cell mass thus reached between 30% to 69% of the normal values, and remained stable for life (see earlier; Supplementary Table 6).

We characterized the δ-cell-derived $insulin^+$ cells at the gene expression level by quantitative polymerase chain reaction (qPCR). We first compared islets isolated 2 weeks after β-cell ablation or after recovery (4 months post-DT) with age-matched control islets. Expression of all the β-cell-specific markers tested was robustly increased in recovered mice (Extended Data Fig. 7b). We also compared regenerated $insulin^+$ cells with native β-cells using sorted $mCherry^+$ cells obtained from either recovered or unablated age-matched (4.5-month-old) *insulin-mCherry; RIP-DTR* mice (Extended Data Fig. 7c). The two cell populations were very similar (Extended Data Fig. 7d), yet the δ-cell-derived replicating β-cells displayed a potent downregulation of cyclin-dependent kinase

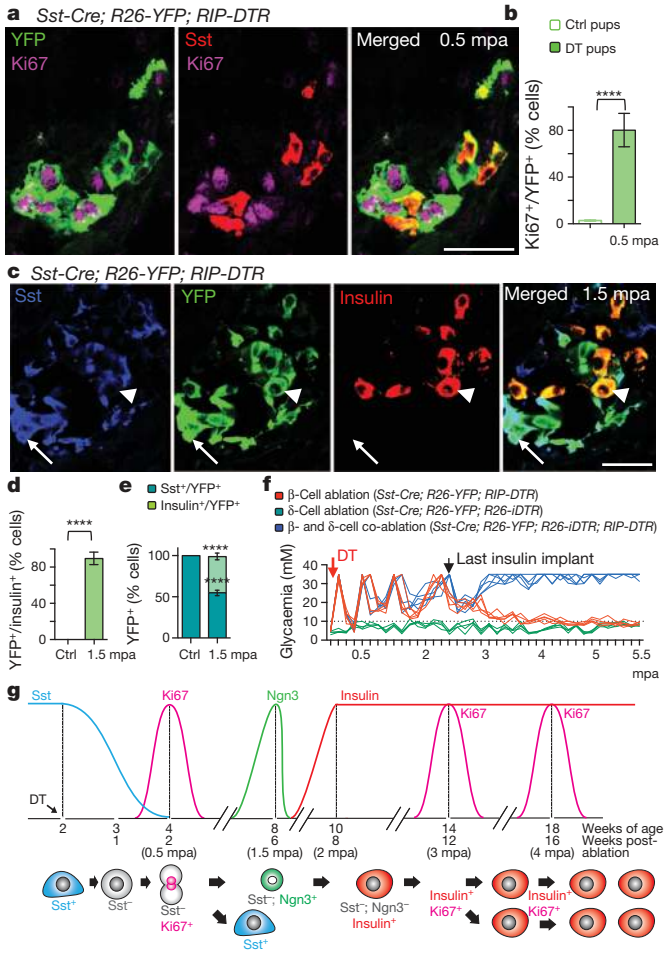

Figure 2 | δ-cells dedifferentiate, proliferate and reprogram into insulin production after extreme β-cell loss in *Sst-Cre; R26-YFP; RIP-DTR* juvenile mice. **a**, Immunofluorescence for YFP and Ki67 at 0.5 mpa. **b**, Eighty per cent of Sst-traced YFP$^+$ cells are Ki67$^+$ after β-cell ablation (controls: $n = 6$; 2,754 YFP$^+$-cells scored; DT: $n = 6$; 3,146 YFP$^+$-cells scored; $P < 0.0001$, Welch's test; $P = 0.0022$, Mann–Whitney). Ctrl, control. **c**, **d**, At 1.5 mpa, 90% of insulin$^+$ cells co-express YFP (controls: $n = 3$; 6,480 insulin$^+$-cells scored; DT: $n = 7$; 1,592 insulin$^+$-cells scored; $P < 0.0001$, Welch's test; $P = 0.0167$, Mann–Whitney). Arrow indicates YFP$^+$/Sst$^+$ cells; arrowhead indicates YFP$^+$/insulin$^+$ cells. **e**, In controls, 99.9% of the YFP$^+$ cells are Sst$^+$ ($n = 3$; 1,673 YFP$^+$-cells scored). In contrast, at 1.5 mpa only 55% of the YFP$^+$ cells are Sst$^+$, while 45% of the YFP$^+$ cells are insulin$^+$ ($n = 5$; 2,295 YFP$^+$-cells scored; $P < 0.0001$, Welch's test; $P = 0.0357$, Mann–Whitney). **f**, Comparative evolution of glycaemia after β-cell ($n = 5$), δ-cell ($n = 4$) and β- and δ-cell co-ablation ($n = 5$) in juveniles. **g**, δ-cell conversion sequence. Scale bars, 20 μm. Error bars show standard deviation (s.d.). ****$P < 0.0001$.

inhibitors and regulators (Extended Data Fig. 7e, f). This suggests that reconstituted insulin$^+$ cells are like β-cells with transient proliferation capacity. Future studies will establish whether reconstituted (δ)β-like cells are true equivalents to native β-cells.

qPCR and lineage-tracing analyses on islets isolated from pups at different regeneration time-points, together with *Ngn3* (also known as *Neurog3*) knockout induction after β-cell ablation, revealed that *Ngn3* transcription is required for the δ-to-insulin$^+$ cell conversion to occur (Extended Data Fig. 8a–k and Supplementary Tables 24–29). Of note, the brief expression of *Ngn3* is a feature of islet precursor cells in the embryonic pancreas[4]. Together, these observations are compatible with a model in which β-cell reconstitution after ablation in juveniles occurs following a defined sequence of events: δ-cells dedifferentiate, replicate once, and then half of the progeny activates *Ngn3* expression before insulin production (Fig. 2g). This was tested in a combined double lineage-tracing experiment using *Sst-Cre; R26-Tomato; Ngn3-YFP; RIP-DTR* mice. Six weeks after β-cell ablation, insulin$^+$ cells in juveniles were Tomato$^+$/YFP$^+$ (Extended Data Fig. 8k).

One key reprogramming and cell cycle entry player is FoxO1, a transcription factor whose downregulation triggers *Ngn3* expression in human fetal pancreatic explants[5] and favours insulin production in Ngn3$^+$ enteroendocrine progenitors[6]. FoxO1, usually in cooperation with TGF-β/SMAD signalling[7,8], inhibits cell proliferation through the transcriptional regulation of cell cycle inhibitors and activators[9], and is involved in cellular senescence[7] (Extended Data Fig. 9a). We next explored the FoxO1 molecular network in purified adult or juvenile δ-cells before and after (1 week) β-cell ablation, using *Sst-Cre; R26-YFP; RIP-DTR* mice.

δ-cells displayed divergent regulation of *Foxo1* in injured juvenile and adult mice. Consistent with *Foxo1* downregulation in juvenile δ-cells, *Pdk1* and *Akt* (also known as *Akt2*) levels were increased, *Cdkn1a* (also known as *p21*) and *Cdkn2b* (also known as *p15Ink4b*) were downregulated, and *Cks1b*, *Cdk2* and *Skp* were upregulated (Fig. 3a), which is compatible with the proliferative capacity of juvenile δ-cells after β-cell ablation. The opposite was found in the δ-cells of ablated adults (Fig. 3a and Extended Data Fig. 9b).

Moreover, in δ-cells of juveniles, but not in adults, there was a robust upregulation of BMP1/4 downstream effectors (Fig. 3b)[10,11]. Inversely, TGF-β pathway genes were upregulated in δ-cells of regenerating adults (Fig. 3b), which is compatible with the senescence scenario[7] involving PI3K/FoxO1 and TGF-β/SMAD cooperation to maintain differentiation and cycle arrest (Extended Data Fig. 9a, b).

In summary, PI3K/AKT and SKP2/SCF pathways potentially cooperate to downregulate *Foxo1* in δ-cells of regenerating juveniles. Also, upregulation of BMP effectors (*Id1* and *Id2*) could contribute to δ-cell dedifferentiation and proliferation, as observed in other systems[10,11] (Fig. 3c). Conversely, the PI3K/AKT pathway remained downregulated in δ-cells of ablated adults, which would allow FoxO1 to impede proliferation and dedifferentiation, probably through partnership with previously described SMADs[12] (Extended Data Fig. 9b).

We next checked whether a transient FoxO1 inhibition in adult mice would lead to a juvenile-like δ-to-β-cell conversion. Indeed, inactivation of FoxO1 in β-cells causes their dedifferentiation[13]. Here, *Sst-Cre; R26-YFP; RIP-DTR* β-cell-ablated adult mice were given a FoxO1 inhibitor (AS1842856) for 1 week, either immediately following ablation (Fig. 3d) or 1 month later (Extended Data Fig. 10f and Supplementary Tables 37–39)[14,15]. While FoxO1 inhibition in non-ablated controls had a minimal effect on insulin expression (Extended Data Fig. 10a–d and Supplementary Tables 30–32), regeneration in diabetic mice was improved: insulin$^+$ cells were more abundant (11-fold; Fig. 3e, f and Supplementary Table 33), and were reprogrammed δ-cells (93% were YFP$^+$, Fig. 3g and Supplementary Table 34). One-fourth of the YFP$^+$ cells expressed insulin only (Fig. 3h, Extended Data Fig. 10e and Supplementary Tables 35, 36), revealing that, like in juveniles, an important fraction of δ-cells had converted to insulin production.

These results support the involvement of a regenerative FoxO1 network and confirm that δ-cell conversion can be pharmacologically induced in diabetic adults. FoxO1 blockade has a pleiotropic effect: inhibition of hepatic gluconeogenesis[14,15] and, as we have shown, promotion of δ-cell reprogramming.

A century ago Morgan coined the terms 'epimorphosis' and 'morphallaxis' to designate, respectively, regeneration involving either cell dedifferentiation and proliferation or direct conversion from one cell type into another without proliferation[16]. Here we report in mammals an age-dependent switch ('adult transition') between epimorphic regeneration during youth, and a less efficient yet persistent throughout life proliferation-independent morphallactic mechanism.

Our findings uncover a novel role for δ-cells; perhaps Sst$^+$ cells in the stomach, intestine or hypothalamus share the same capabilities. Intra-islet cell plasticity triggered by the disappearance of β-cells is influenced by age: the proliferation decline in ageing cells[17] would explain the need for an adult transition. Although less efficient, α-cell plasticity remains long-time after β-cell loss since it is proliferation-independent.

a

Gene name	Fold regulation: Pups (1 wpa pups / 3 wo control)	Fold regulation: Adults (1 wpa pups / 3 wo control)
FoxO1	–2.79×	1.7×
Cyclin inhibitors		
Cdkn1a	–1.77×	3.71×
Cdkn1b	1.34×	–1.01×
Cdkn1c	–1.58×	2.51×
Cdkn2b	–36.81×	14.42×
SCF-complex related		
Skp2	13.45×	–1.57×
Cdk2	14.89×	–1.54×
Cks1b	7.77×	1.003×
PI3K signalling pathway		
PDK1	3.45×	–4.24×
AKT2	1.93×	–1.88×

Upregulated · Not assessed · Downregulated · Unchanged

b

Gene name	Fold regulation: Pups (1 wpa pups / 3 wo control)	Fold regulation: Adults (1 wpa adults / 2 mo control)
TGF-β signalling pathway components		
Eng	–57.36×	3.12×
Tgfb1	–1.24×	8.17×
Tgfb2	22.4×	–2.8×
Tgfb3	–1.33×	1
Tgfb1i1	–2.16×	1
Tgfb1r1	1.21×	23.26×
Tgfb1r2	–135.49×	1
Tgfb1r3	–9.4×	1
Smad2	1.67×	2.20×
Smad4	–1.51×	5.35×
BMP pathway downstream effectors		
Myc	1.55×	1
Id1	44.26×	1
Id2	487.08×	–3.18×
Inhba	22.13×	–2.98×
Smad1	1.54×	1.55×
Smad3	6.1×	–12.38×

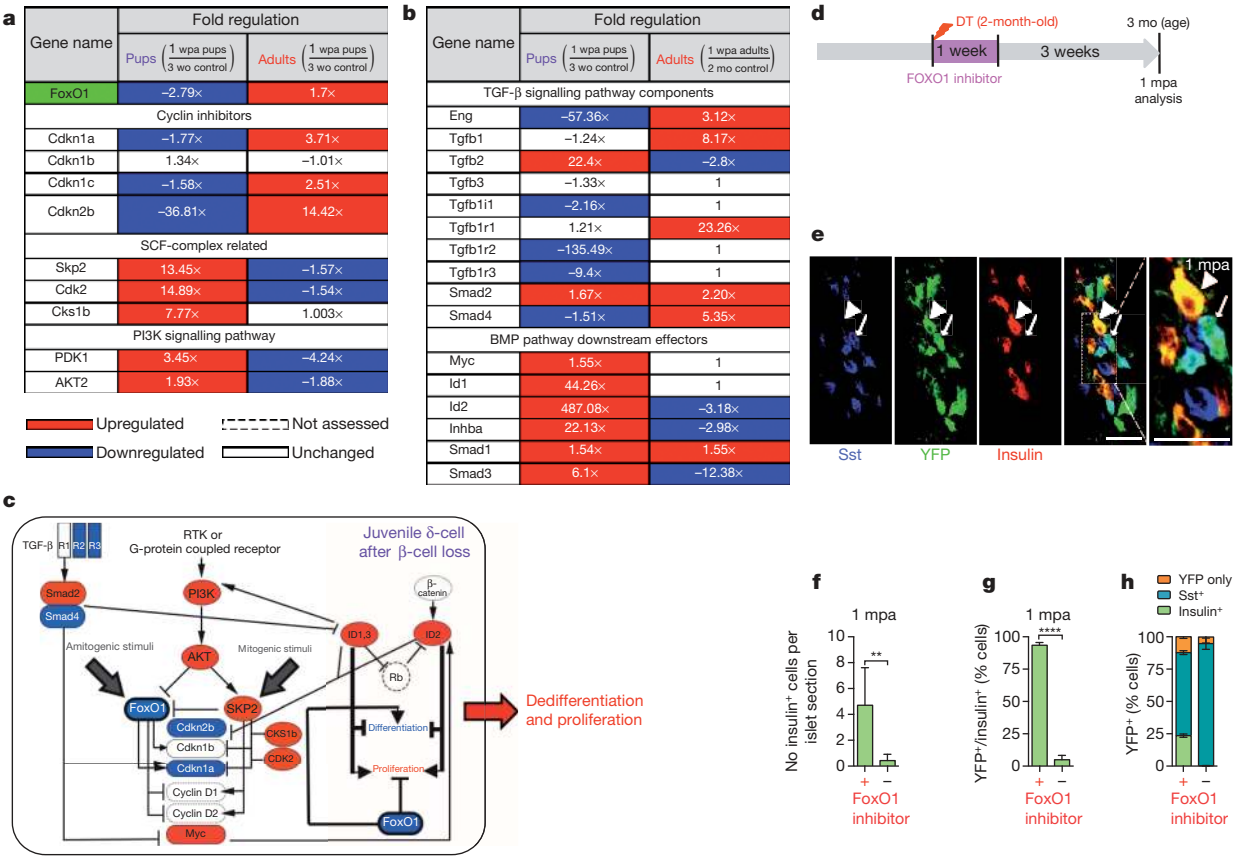

Figure 3 | Age-dependent effect of β-cell loss on δ-cells. **a**, **b**, Transcriptional variation of cell cycle regulators, PI3K/AKT/FoxO1 network genes (**a**), and TGF-β and BMP components and effectors (**b**) in juvenile and adult δ-cells 1 week after ablation, as compared with age-matched controls. wpa, weeks post-ablation. **c**, β-cell loss before puberty triggers FoxO1 downregulation in δ-cells, while the opposite occurs in adults (see Extended Data Fig. 9b). **d**, Experimental design to transiently inhibit FoxO1 in β-cell-ablated adult mice. **e**, Induction of δ-to-insulin cell conversion in diabetic adult mice. Dashed box indicates the area that is magnified in the right-most panel. Arrowheads indicate a converted δ-cell, which has lost Sst expression (insulin$^+$ and YFP$^+$ cell). Arrows point to an unaffected δ-cell, which is Sst$^+$ and YFP$^+$, and does not express insulin. Scale bars, 20 μm. **f**, **g**, Insulin$^+$ cells are 11-fold more abundant in FoxO1 inhibitor-treated mice (treated: $n = 190$ islets, 4 mice; untreated: $n = 95$ islets, 3 mice (inter-islet $P < 0.0001$, inter-individual $P = 0.0065$, Welch's test; $P < 0.0001$, Mann–Whitney) (**f**), and they are YFP$^+$ (93%) (treated: $n = 4$; 894 insulin$^+$-cells scored; untreated: $n = 6$; 370 insulin$^+$-cells scored; $P < 0.0001$, Welch's test; $P = 0.0095$, Mann–Whitney) (**g**). **h**, One-fourth of δ-(YFP$^+$) cells in adult β-cell-ablated FoxO1-inhibited mice dedifferentiate and become insulin expressers (treated: $n = 4$; 3,358 YFP$^+$-cells scored; untreated: $n = 6$; 2,559 YFP$^+$-cells scored). Error bars show s.d. $^{**}P < 0.01$; $^{****}P < 0.0001$.

These phenomena might be translatable to humans, as there is efficient β-cell regeneration in children with type 1 diabetes or after pancreatectomy[9,18,19], and glucagon/insulin bihormonal human cells have been described upon epigenetic manipulation *ex vivo*[20], and in diabetic patients[21,22]. Knowing also that only a small fraction of the α-cell population is sufficient to maintain glucagon signalling[23], understanding the nature of the diverse forms of intra-islet cell conversion might provide new opportunities for fostering the formation of (α)β-like and (δ)β-like cells.

Online Content Methods, along with any additional Extended Data display items and Source Data, are available in the online version of the paper; references unique to these sections appear only in the online paper.

Received 15 July 2013; accepted 30 June 2014.
Published online 20 August 2014.

1. Matveyenko, A. V. & Butler, P. C. Relationship between β-cell mass and diabetes onset. *Diabetes Obes. Metab.* **10** (suppl. 4), 23–31 (2008).
2. Atkinson, M. A. The pathogenesis and natural history of type 1 diabetes. *Cold Spring Harb. Perspect. Med.* http://dx.doi.org/10.1101/cshperspect.a007641 (2012).
3. Thorel, F. *et al.* Conversion of adult pancreatic α-cells to β-cells after extreme β-cell loss. *Nature* **464,** 1149–1154 (2010).
4. Desgraz, R. & Herrera, P. L. Pancreatic neurogenin 3-expressing cells are unipotent islet precursors. *Development* **136,** 3567–3574 (2009).
5. Al-Masri, M. *et al.* Effect of forkhead box O1 (FOXO1) on β cell development in the human fetal pancreas. *Diabetologia* **53,** 699–711 (2010).
6. Talchai, C., Xuan, S., Kitamura, T., DePinho, R. A. & Accili, D. Generation of functional insulin-producing cells in the gut by Foxo1 ablation. *Nature Genet.* **44,** 406–412 (2012).
7. Muñoz-Espín, D. *et al.* Programmed cell senescence during mammalian embryonic development. *Cell* **155,** 1104–1118 (2013).
8. Seoane, J., Le, H. V., Shen, L., Anderson, S. A. & Massague, J. Integration of Smad and Forkhead pathways in the control of neuroepithelial and glioblastoma cell proliferation. *Cell* **117,** 211–223 (2004).
9. Karges, B. *et al.* Immunological mechanisms associated with long-term remission of human type 1 diabetes. *Diabetes Metab. Res. Rev.* **22,** 184–189 (2006).
10. Yokota, Y. Id and development. *Oncogene* **20,** 8290–8298 (2001).
11. Perk, J., Iavarone, A. & Benezra, R. Id family of helix-loop-helix proteins in cancer. *Nature Rev. Cancer* **5,** 603–614 (2005).
12. van der Vos, K. E. & Coffer, P. J. FOXO-binding partners: it takes two to tango. *Oncogene* **27,** 2289–2299 (2008).
13. Talchai, C., Xuan, S., Lin, H. V., Sussel, L. & Accili, D. Pancreatic β cell dedifferentiation as a mechanism of diabetic β cell failure. *Cell* **150,** 1223–1234 (2012).
14. Nagashima, T. *et al.* Discovery of novel forkhead box O1 inhibitors for treating type 2 diabetes: improvement of fasting glycemia in diabetic db/db mice. *Mol. Pharmacol.* **78,** 961–970 (2010).
15. Tanaka, H. *et al.* Effects of the novel Foxo1 inhibitor AS1708727 on plasma glucose and triglyceride levels in diabetic db/db mice. *Eur. J. Pharmacol.* **645,** 185–191 (2010).
16. Morgan, T. H. Regeneration and liability to injury. *Science* **14,** 235–248 (1901).
17. Chen, H. *et al.* PDGF signalling controls age-dependent proliferation in pancreatic β-cells. *Nature* **478,** 349–355 (2011).
18. Karges, B. *et al.* Complete long-term recovery of β-cell function in autoimmune type 1 diabetes after insulin treatment. *Diabetes Care* **27,** 1207–1208 (2004).

19. Desgraz, R., Bonal, C. & Herrera, P. L. β-Cell regeneration: the pancreatic intrinsic faculty. *Trends Endocrinol. Metab.* **22,** 34–43 (2011).
20. Bramswig, N. C. *et al.* Epigenomic plasticity enables human pancreatic alpha to beta cell reprogramming. *J. Clin. Invest.* **123,** 1275–1284 (2013).
21. Butler, A. E. *et al.* Marked expansion of exocrine and endocrine pancreas with incretin therapy in humans with increased exocrine pancreas dysplasia and the potential for glucagon-producing neuroendocrine tumors. *Diabetes* **62,** 2595–2604 (2013).
22. Yoneda, S. *et al.* Predominance of β-cell neogenesis rather than replication in humans with an impaired glucose tolerance and newly diagnosed diabetes. *J. Clin. Endocrinol. Metab.* **98,** 2053–2061 (2013).
23. Thorel, F. *et al.* Normal glucagon signaling and β-cell function after near-total α-cell ablation in adult mice. *Diabetes* **60,** 2872–2882 (2011).

Supplementary Information is available in the online version of the paper.

Acknowledgements We are grateful to D. Belin, P. Vassalli, R. Stein, A. Cookson, A. Ruiz i Altaba, M. González Gaitán, B. Galliot and I. Rodríguez for comments, support and discussions, and to G. Gallardo, O. Fazio, K. Hammad and B. Polat for technical help. We thank G. Gradwohl for the *Ngn3-YFP* mice. F.M.G. and F.R. were funded by Wellcome Trust grants WT088357/Z/09/Z and WT084210/Z/07/Z, respectively. This work was funded with grants from the National Institutes of Health/National Institute of Diabetes and Digestive and Kidney Diseases (Beta Cell Biology Consortium), the Juvenile Diabetes Research Foundation and the Swiss National Science Foundation (NRP63) to P.L.H.

Author Contributions S.C. conceived and performed the experiments and analyses, and wrote the manuscript. F.M.G. and F.R. generated the *Sst-Cre* line, and G.G. and J.N.J. generated the *Ngn3-CreERT, Ngn3-tTA* and *TRE-Ngn3* lines. D.B. characterized the pancreatic expression of the *Sst-Cre* line and performed the adult analysis. L.G. performed experiments and analyses. V.C. profiled sorted fluorescent adult islet cells. K.F. and F.T. performed immunofluorescence microscopy. P.L.H. conceived the experiments and wrote the manuscript.

Author Information Reprints and permissions information is available at www.nature.com/reprints. The authors declare no competing financial interests. Readers are welcome to comment on the online version of the paper. Correspondence and requests for materials should be addressed to P.H. (pedro.herrera@unige.ch).

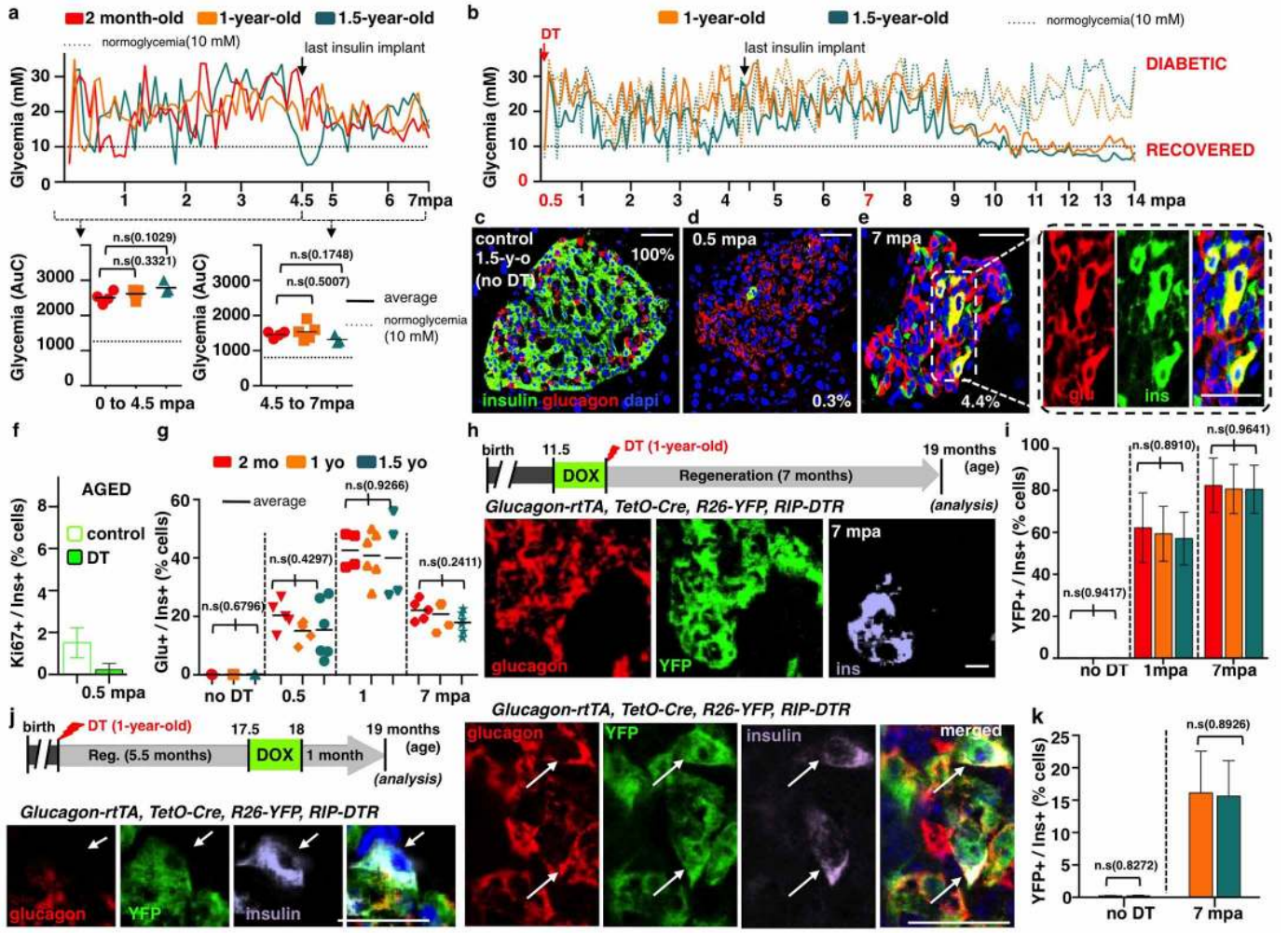

Extended Data Figure 1 | Maintenance of α-cell plasticity in diabetic aged mice. **a**, Evolution of glycaemia in β-cell-ablated adults (middle-aged) and aged mice. The area under the curve (AuC) in middle-aged (2-month-old, $n = 4$) and aged (1- and 1.5-year-old, $n = 5$ and $n = 3$) mice before and after stopping insulin administration revealed no statistical difference between groups (Welch's test, $P_{0–4.5\,mpa} = 0.1029, 0.3321$; $P_{4.5–7\,mpa} = 0.1748, 0.5007$; one-way analysis of variance (ANOVA), $P = 0.1161$, $P = 0.2681$; and Mann–Whitney, $P = 0.1640, 0.4519$). **b**, Evolution of glycaemia in 14 aged mice over a period of 14 months post-ablation (mpa). Mice were treated with insulin for 4.5 months; most of them (5/7 in each group) subsequently recovered from diabetes. **c**–**e**, Pancreatic islets before (**c**) and after (**d**, **e**) β-cell ablation in 1.5-year-old mice; β-cell mass increases 3.5-fold between 0.5 and 1 mpa, 12-fold at 7 mpa and 32-fold at 14 mpa, in all age groups. Percentages (0.3% and 4.4%) indicate β-cell mass relative to unablated controls (Supplementary Table 1). Two-month-old: $n_{0.5\,mpa} = 4$; $n_{1\,mpa} = 4$; $n_{7\,mpa} = 4$; 1-year-old: $n_{0.5\,mpa} = 5$, $n_{1\,mpa} = 5$, $n_{7\,mpa} = 5$, $n_{14\,mpa} = 8$; 1.5-year-old: $n_{0.5\,mpa} = 3$; $n_{1\,mpa} = 3$; $n_{7\,mpa} = 3$, $n_{14\,mpa} = 8$. **f**, β-Cell proliferation is very low in aged mice, whether control (1.5%; $n = 8$; 39,790 insulin$^+$-cells scored) or ablated (0.2%; $n = 6$; 938 insulin$^+$-cells scored) (Supplementary Table 2). **g**, Proportion of insulin$^+$ cells also containing glucagon after DT is not different between groups (Supplementary Table 3). Control: $n_{2\text{-month-old}} = 3$; $n_{1\text{-year-old}} = 3$; $n_{1.5\text{-year-old}} = 3$; 0.5 mpa: $n_{2\text{-month-old}} = 5$; $n_{1\text{-year-old}} = 5$; $n_{1.5\text{-year-old}} = 6$; 1 mpa: $n_{2\text{-month-old}} = 4$; $n_{1\text{-year-old}} = 6$; $n_{1.5\text{-year-old}} = 4$; 7 mpa: $n_{2\text{-month-old}} = 5$; $n_{1\text{-year-old}} = 5$; $n_{1.5\text{-year-old}} = 6$. One-way ANOVA ($P = 0.6796, 0.4297, 0.9266, 0.2411$); note that 40% of the cells containing insulin at 1 mpa also contained glucagon. The proportion of glucagon$^+$/insulin$^+$ cells remains constant between 0.5 and 7 mpa, while the number of insulin$^+$ cells increases with time (**e**; Supplementary Table 1), suggesting that there is a cumulative recruitment of α-cells into insulin production. **h**, Islet with YFP$^+$/glucagon$^+$/insulin$^+$ cells in 1-year-old *glucagon-rtTA; TetO-Cre; R26-YFP; RIP-DTR* mice, 7 mpa; rtTA expression allows the selective irreversible YFP labelling of adult α-cells upon administration of doxycycline (DOX) before β-cell ablation. **i**, Proportion of YFP-labelled insulin-expressing cells in DOX-treated mice. Eighty per cent of insulin$^+$ cells are YFP$^+$ after 7 mpa, in all age groups (Supplementary Table 4). Control: $n_{2\text{-month-old}} = 3$; $n_{1\text{-year-old}} = 3$; $n_{1.5\text{-year-old}} = 3$; 1 mpa: $n_{2\text{-month-old}} = 5$; $n_{1\text{-year-old}} = 3$; $n_{1.5\text{-year-old}} = 3$; 7 mpa: $n_{2\text{-month-old}} = 5$; $n_{1\text{-year-old}} = 5$; $n_{1.5\text{-year-old}} = 5$. One-way ANOVA ($P = 0.9417, 0.8910, 0.9641$). **j**, **k**, YFP$^+$/glucagon$^+$/insulin$^+$ cells at 7 mpa, following DOX pulse-labelling at 5.5 months after β-cell loss (Supplementary Table 5). Control: $n_{1\text{-year-old}} = 5$; $n_{1.5\text{-year-old}} = 5$; 7 mpa: $n_{1\text{-year-old}} = 5$; $n_{1.5\text{-year-old}} = 5$; Welch's correction ($P = 0.8272, 0.8926$), Mann–Whitney ($P = 0.9444$). On average, 15% of the insulin$^+$ cells found were YFP labelled, some of which no longer contained glucagon as in **j**, bottom row. Note the decreased proportion of YFP-labelled insulin$^+$ cells when α-cells are tagged late after ablation (from 80% to 15%; compare **i** and **k**), and the presence of YFP-labelled insulin$^+$/glucagon-negative cells in the latter situation (**j**), suggesting that bihormonal α-cells slowly but gradually lose glucagon gene activity. Scale bars, 20 μm. Error bars show s.d.

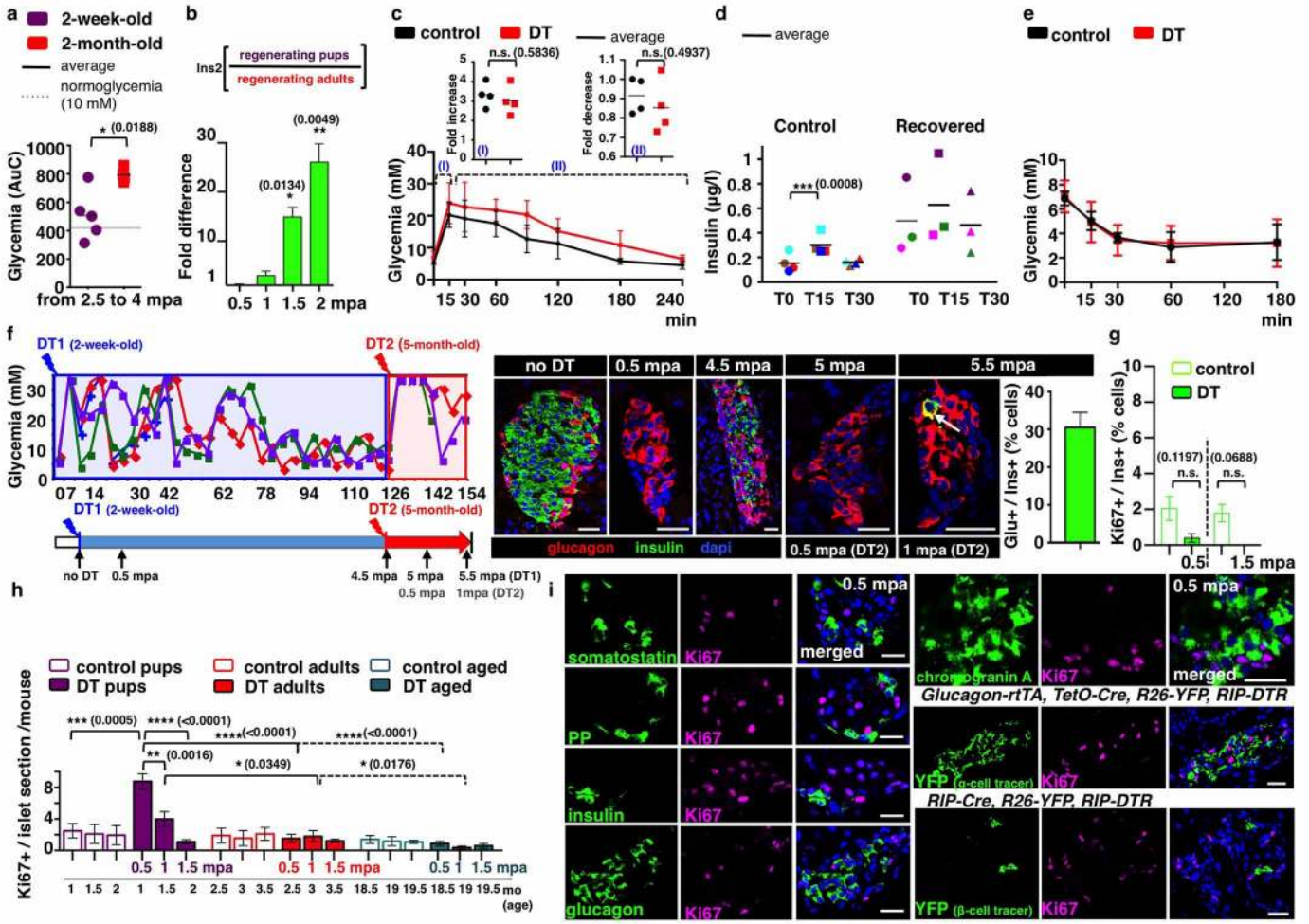

Extended Data Figure 2 | Diabetes recovery in pre-pubertal mice. **a**, Evolution of glycemia (AuC) between 2.5 and 4 mpa, in pups and adults (see Fig. 1b) (Welch's test, $P = 0.0188$). **b**, qPCR of insulin 2 messenger RNA after β-cell ablation; insulin 2 transcripts are 25-fold more abundant in pups than in adults at 2 mpa ($n = 3$ mice per group, each individual sample was run in triplicate in each reaction for a total of three independent reactions). Built-in Welch's test ($P = 0.0134, 0.0049$). Error bars show s.d. **c**, Glucose tolerance tests (IPGTT) for DT-treated (4.5 mpa, $n = 4$) and age-matched controls ($n = 4$); note the fold increase between glucose injection and the glycaemic peak during IPGTT for each animal, and fold decrease between glycaemic peak and T120 (two-tailed unpaired t-test, $P_I = 0.5836$, $P_{II} = 0.4937$). **d**, Plasma insulin at time point (in min) T0, T15 and T30 during the IPGTT. Control: $n = 4$; DT: $n = 4$; two-tailed paired t-test ($P = 0.0008$). **e**, Insulin tolerance tests (ITT) performed 1.5 years after β-cell ablation at 2 weeks of age. Controls: $n = 7$; DT: $n = 10$. **f**, 4.5 months after β-cell ablation (at 2 weeks), three mice became normoglycaemic and received a second treatment with DT. Ablation of regenerated insulin$^+$ cells in recovered mice leads to the appearance of glucagon$^+$/insulin$^+$ cells, corresponding to the type of 'α-cell-dependent' regeneration observed in adults (31% of insulin$^+$ cells also contained glucagon; Supplementary Table 8). Arrow indicates glucagon$^+$/insulin$^+$ bihormonal cell. Error bars show standard error of the mean (s.e.m.). **g**, β-cell proliferation is very low in regenerating pups (Supplementary Table 9). Control: $n_{1\text{-month-old}} = 3$, 6,006 insulin$^+$-cells scored; $n_{2\text{-month-old}} = 3$, 6,358 insulin$^+$-cells scored; DT: $n_{0.5\,mpa} = 5$, 412 insulin$^+$-cells scored; $n_{1.5\,mpa} = 3$, 675 insulin$^+$-cells scored; Welch's test ($P = 0.1197$, $P = 0.0688$). Error bars show s.e.m. **h**, Islet cell proliferation is increased (3.5-fold; Ki67$^+$ cells) in islets of DT-treated pups at 0.5 mpa. Control: $n_{1\text{-month-old}} = 3$, 95 islets scored; $n_{1.5\text{-month-old}} = 3$, 94 islets scored; $n_{2\text{-month-old}} = 3$, 90 islets scored; $n_{2.5\text{-month-old}} = 3$, 89 islets scored; $n_{3\text{-month-old ctrl}} = 3$, 91 islets scored; $n_{3.5\text{-month-old}} = 3$, 93 islets scored; $n_{18.5\text{-month-old}} = 3$, 83 islets scored; $n_{19\text{-month-old ctrl}} = 3$, 83 islets scored; $n_{19.5\text{-month-old}} = 3$, 88 islets scored; DT (2-week-old): $n_{0.5\,mpa} = 6$, 333 islets scored; $n_{1\,mpa} = 3$, 91 islets scored; $n_{1.5\,mpa} = 3$, 90 islets scored; DT (2-month-old): $n_{0.5\,mpa} = 3$, 76 islets scored; $n_{1\,mpa} = 3$, 77 islets scored; $n_{1.5\,mpa} = 3$, 81 islets scored; DT (1.5-year-old): $n_{0.5\,mpa} = 3$, 74 islets scored; $n_{1\,mpa} = 3$, 81 islets scored; $n_{1.5\,mpa} = 3$, 77 islets scored. Error bars show s.d. Welch's test, one-way ANOVA ($P < 0.001$), Mann–Whitney ($P = 0.0238$). **i**, Ki67$^+$ cells are hormone, chromogranin-A-negative; lineage-traced α- and DT-spared β-cells are Ki67-negative. Scale bars, 20 µm.

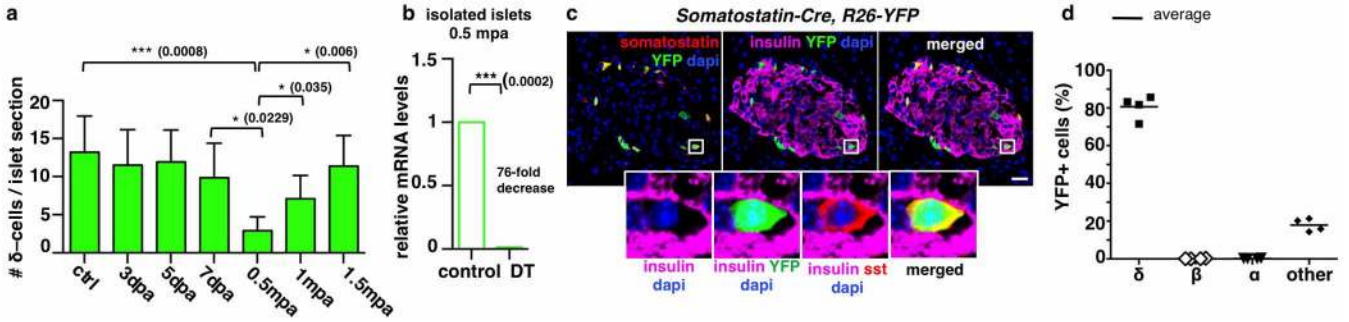

Extended Data Figure 3 | δ-cell labelling and tracing in transgenic mice. **a**, The number of Sst^+ cells transiently decreases by 80% during the second week after ablation. $n_{control} = 255$ islets, 7 mice; $n_{3\,dpa} = 240$ islets, 5 mice; $n_{5\,dpa} = 228$ islets, 5 mice; $n_{7\,dpa} = 251$ islets, 5 mice; $n_{0.5\,mpa} = 267$ islets, 6 mice; $n_{1\,mpa} = 266$ islets, 5 mice; $n_{1.5\,mpa} = 206$ islets, 5 mice. Error bars show s.d. Welch's test ($P = 0.0008$, 0.0229, 0.006, 0.035), one-way ANOVA ($P < 0.0001$), Mann–Whitney ($P = 0.0043$). **b**, Relative *Sst* gene expression sharply decreases 2 weeks after β-cell ablation in 2-week-old mice ($n = 3$ mice per group, each individual sample of each experimental group was run in triplicate, in three independent reactions). Built-in Welch's test ($P = 0.0002$). Error bars show s.d. **c**, *Sst-Cre; R26-YFP* mice. Cre activity efficiently and specifically occurs in δ-cells (box: enlarged cell). Scale bar, 20 μm. **d**, Quantitative values of reporter gene expression in islet cells ($n = 4$; 1,263 YFP^+-cells scored).

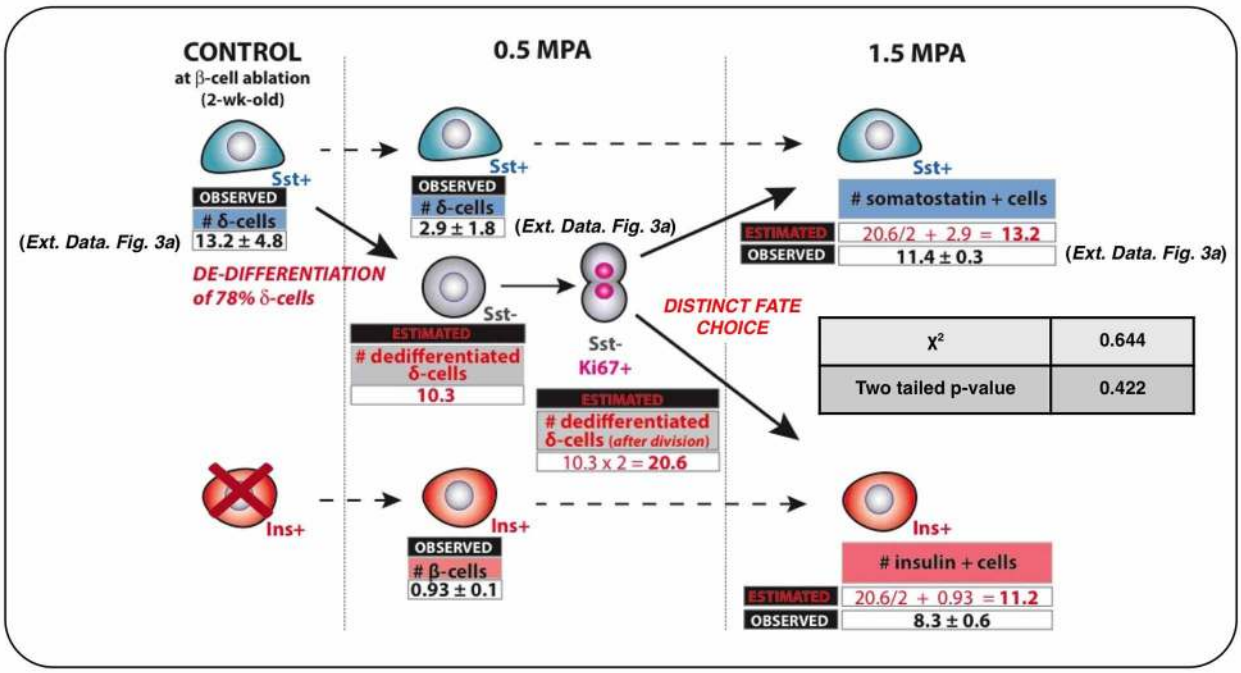

Extended Data Figure 4 | δ-cells dedifferentiate, proliferate and reprogram into insulin production after extreme β-cell loss in juvenile mice. Observed and expected numbers of Sst^+ and $insulin^+$ cells per islet section, before and after β-cell ablation. Cells scored after 6 weeks (Extended Data Fig. 3a) correspond (χ^2 test) with estimates made assuming that dedifferentiated proliferating δ-cells yield two types of progeny (as deduced from Fig. 2c, e). Dashed arrows indicate phenotypic stability; plain arrows indicate dynamic behaviour (dedifferentiation and replication).

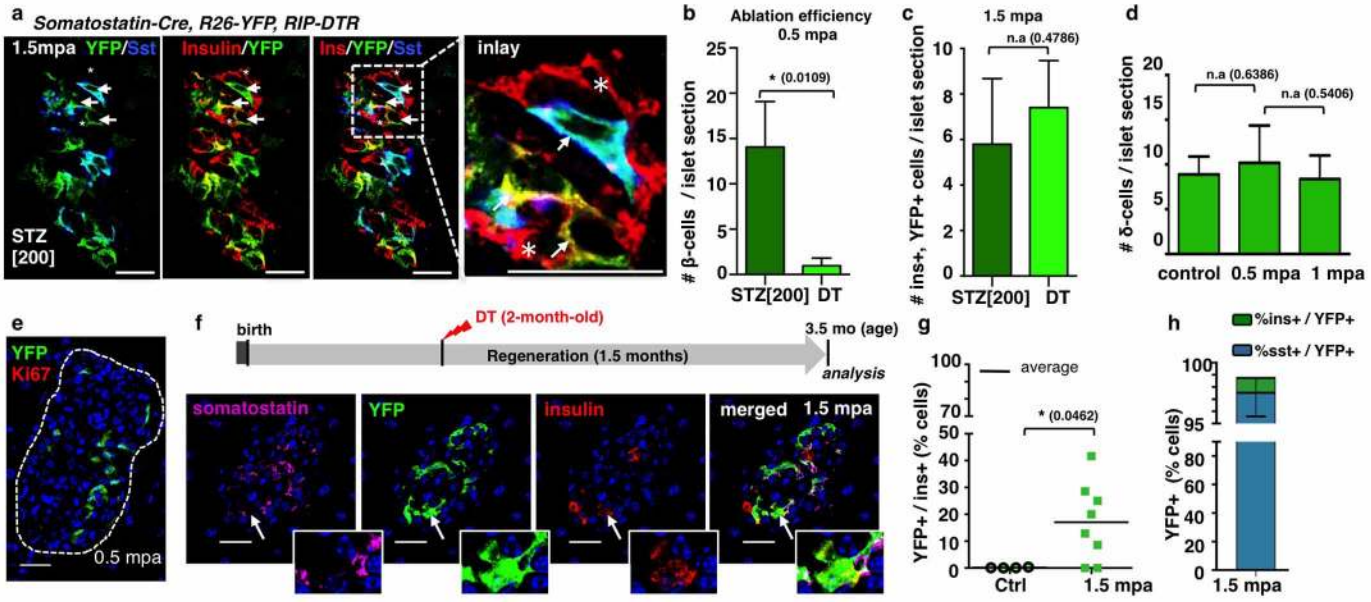

Extended Data Figure 5 | Regeneration in streptozotocin-treated pups and DT-treated adults. **a**, Immunofluorescence showing YFP-labelled insulin$^+$ cells at 1.5 month following streptozotocin (STZ)-induced ablation of β-cells in 2-week-old mice. Arrows indicate YFP$^+$/insulin$^+$ cells; arrowhead indicates YFP$^+$/Sst$^+$ cell; asterisks indicate escaping β-cells. **b**, Number of remaining β-cells per islet section at 2 weeks after streptozotocin or DT treatment in pups, reflecting difference in ablation efficiency of the two methods (Supplementary Table 18). $n_{STZ} = 87$ islets, 3 mice; $n_{DT} = 361$ islets, 4 mice. Welch's test (inter-islet $P < 0.0001$; inter-individual $P = 0.0109$), Mann–Whitney ($P < 0.001$). **c**, The number of YFP$^+$/insulin$^+$ cells per islet section at 1.5 mpa is not significantly different between the two β-cell ablation methods (Supplementary Table 19). $n_{STZ} = 88$ islets, 3 mice; $n_{DT} = 193$ islets, 7 mice. Welch's test ($P = 0.4786$). **d**, δ-cell numbers per islet section in controls ($n = 3$, 174 islets scored), 0.5 mpa ($n = 4$, 140 islets scored) and 1 mpa ($n = 3$, 86 islets scored). Unpaired *t*-test, two-tailed ($P = 0.6386$; $P = 0.5406$). **e**, Immunofluorescence for YFP and Ki67 2 weeks (0.5 mpa) after DT, in *Sst-Cre; R26-YFP; RIP-DTR* mice. **f**, Experimental design for δ-cell tracing in β-cell-ablated *Sst-Cre; R26-YFP; RIP-DTR* mice at 2 months of age, and immunofluorescence for Sst, YFP and insulin at 1.5 mpa. Arrow indicates YFP$^+$/insulin$^+$/Sst$^-$ cell. **g**, At 1.5 mpa, 17% of insulin$^+$ cells co-express YFP versus almost 100% in ablated prepubescent mice. Control: $n = 4$; DT: $n = 8$; unpaired *t*-test, two-tailed ($P = 0.0462$). **h**, At 1.5 mpa, 98% of the YFP$^+$ cells are Sst$^+$, and 1% are insulin$^+$ cells (versus 44% in mice ablated before puberty; $n = 8$, unpaired *t*-test, two-tailed). Scale bars, 20 μm. Error bars show s.d.

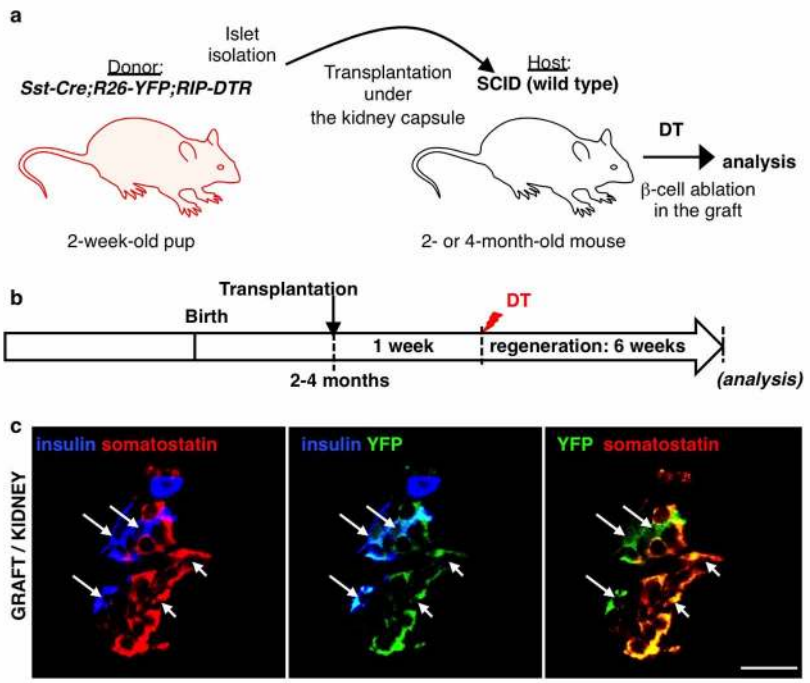

Extended Data Figure 6 | δ-to-β-cell conversion after β-cell ablation is maintained in young islets ablated underneath the kidney capsule of adult hosts. **a**, Islet transplantation design: 400–600 islets isolated from 2-week-old *Sst-Cre; R26-YFP; RIP-DTR* transgenics were transferred under the kidney capsule of 2-month-old immunodeficient (SCID) mice ($n = 3$). **b**, Experimental design: after 1 week of engraftment, adult host mice were DT-treated and left to regenerate for 6 weeks. **c**, δ-to-β conversion was observed in β-cell-ablated engrafted islets, like in the pancreas of juvenile mice. Scale bars, 20 μm.

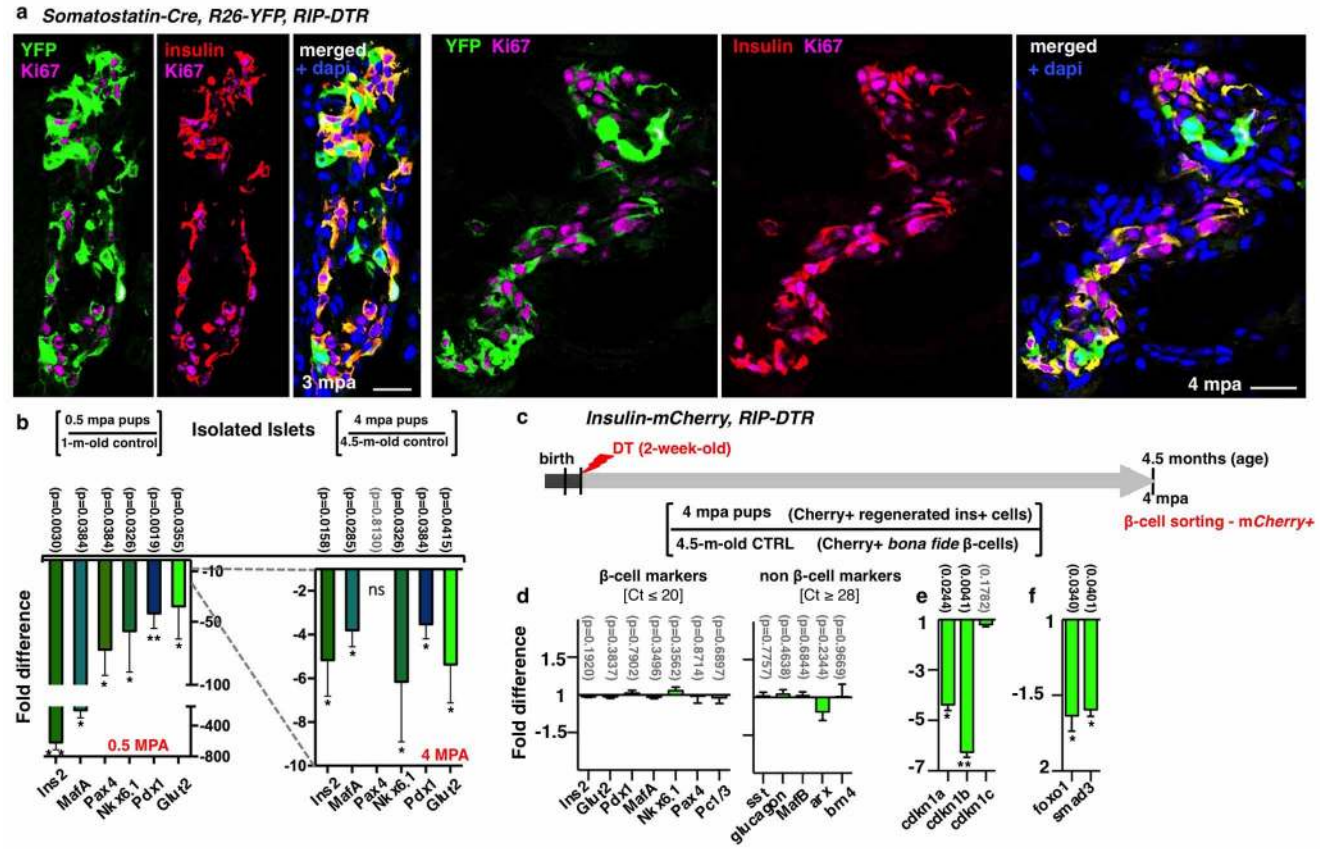

Extended Data Figure 7 | Characterization of δ-cell-derived regenerated insulin$^+$ cells. **a**, Once differentiated from δ-cells (YFP$^+$), the newly formed β-cells re-enter the cell cycle (Ki67$^+$ cells). Two waves of massive replication occur, at 3 and 4 months after injury, respectively (Supplementary Table 23). **b**, qPCR for β-cell-specific genes using RNA extracted from islets isolated from control and DT-treated mice, either 2 weeks or 4 months after DT administration (0.5 mpa and 4 mpa). Note that after an initial extreme downregulation of all the β-cell-specific markers explored, their levels significantly recover after 4 months, which correlates with the observed robust regeneration and diabetes recovery. Values represent the ratio between each regeneration time-point and its age-matched control. **c**, Experimental design. **d**, qPCR comparison between regenerated mCherry$^+$/insulin$^+$ cells isolated from mice 4 months after β-cell ablation, and mCherry$^+$ β-cells obtained from age-matched controls (4.5-month-old). All markers tested are expressed at identical levels in both groups; non-β-cell markers are expressed at extremely reduced levels (threshold cycle (CT) ranging from 28 to 31), showing the same degree of purity in both types of cell preparations. **e**, **f**, Interestingly, in contrast to bona fide β-cells isolated from 4.5-month-old controls, regenerated insulin$^+$ cells have lower levels of cyclin-dependent kinase inhibitors, FoxO1 and Smad3. This correlates with their increased proliferative capacity at this specific time-point. Scale bars, 20 μm. qPCRs: $n = 3$ mice per group; each individual sample of each experimental group was run in triplicate, in three independent reactions; built-in Welch's test. Error bars show s.d.

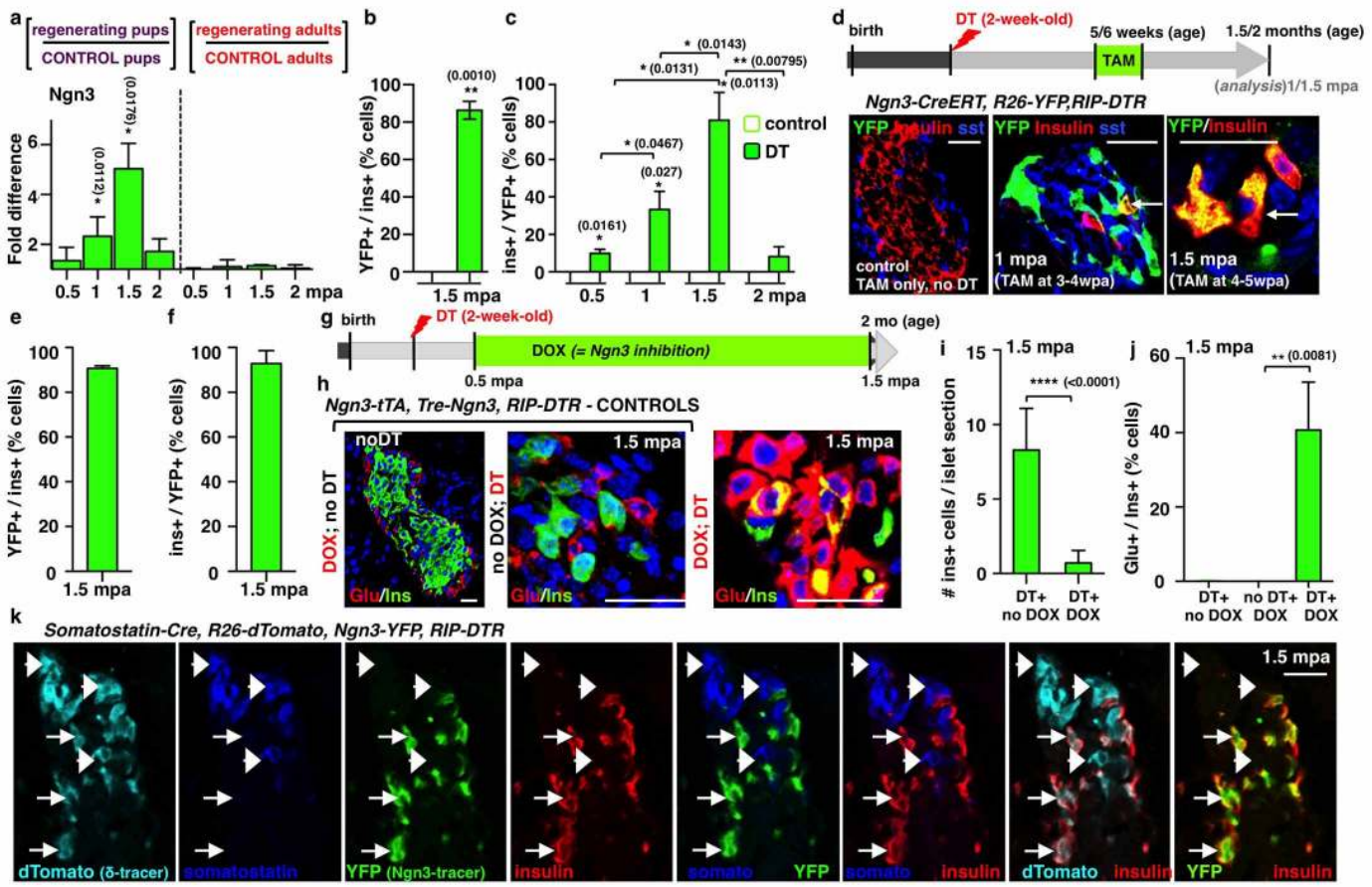

Extended Data Figure 8 | Ngn3 activation is required for insulin expression in dedifferentiated δ-cells. **a**, qPCR for *Ngn3* mRNA after β-cell ablation reveals a transitory fivefold upregulation of *Ngn3* transcripts 6 weeks after β-cell ablation when β-cell ablation is performed before puberty, but not in adult mice. Controls: $n_{1\text{-month-old}} = 3$; $n_{1.5\text{-month-old}} = 3$; $n_{2\text{-month-old}} = 6$; $n_{2.5\text{-month-old}} = 3$; $n_{2.5\text{-month-old}} = 3$; $n_{3\text{-month-old}} = 3$; $n_{3.5\text{-month-old}} = 3$; $n_{4\text{-month-old}} = 3$; DT (2-week-old): $n_{0.5\text{ mpa}} = 3$; $n_{1\text{ mpa}} = 3$; $n_{1.5\text{ mpa}} = 6$; $n_{2\text{ mpa}} = 3$; DT (2-month-old): $n_{0.5\text{ mpa}} = 3$; $n_{1\text{ mpa}} = 3$; $n_{1.5\text{ mpa}} = 3$; $n_{2\text{ mpa}} = 3$. Each individual sample (mouse) was run in triplicate, in each of three independent reactions. Built-in Welch's test ($P = 0.0112$, 0.0178). **b**, *Ngn3* transcriptional activity can be monitored in *Ngn3-YFP* knock-add-on mice because *Ngn3* promoter activity results in YFP expression. In non-ablated age-matched control pups, or in ablated adults, no islet YFP$^+$ cells were found (data not shown), yet when β-cells are ablated at 2 weeks of age, 86% of insulin$^+$ cells also express YFP$^+$ at 1.5 mpa. Control: $n = 3$, 6,358 insulin$^+$-cells scored; DT: $n = 3$, 675 insulin$^+$-cells scored; Welch's test ($P = 0.0010$). **c**, At 1.5 mpa, 81% of YFP$^+$ cells co-express insulin, but no glucagon, Sst or PP (data not shown). Two weeks later, YFP$^+$ cells are almost absent, reflecting the downregulation of Ngn3 expression reported in **a**, and suggesting that insulin$^+$ cells originate from cells transiently activating Ngn3 expression after ablation. Control: $n_{1\text{-month-old}} = 3$; $n_{1.5\text{-month-old}} = 3$; $n_{2\text{-month-old}} = 3$; $n_{2.5\text{-month-old}} = 3$; absent YFP$^+$ cells in all control conditions; DT: $n_{0.5\text{ mpa}} = 3$, 31 YFP$^+$ cells; $n_{1\text{ mpa}} = 3$, 123 YFP$^+$ cells; $n_{1.5\text{ mpa}} = 3$, 729 YFP$^+$ cells; $n_{2\text{ mpa}} = 3$; 47 YFP$^+$ cells. Welch's test and ANOVA ($P < 0.0001$). **d**, Irreversible lineage tracing of Ngn3-expressing cells at 1 and 1.5 mpa upon tamoxifen (TAM) administration in *Ngn3-CreERT; R26-YFP; RIP-DTR* mice; immunofluorescence analyses reveal that in the absence of β-cell ablation, there is no YFP induction (controls). In ablated mice, nearly all insulin$^+$ cells are YFP$^+$ with time (arrows). At early time-points (1 mpa), YFP$^+$/hormone-negative cells are found: these are probably differentiating cells before insulin expression. **e**, **f**, In β-cell-ablated *Ngn3-CreERT; R26-YFP; RIP-DTR* pups, 91% of insulin$^+$ cells co-express YFP$^+$ (control: $n = 3$, 3,472 insulin$^+$-cells scored, DT: $n = 3$, 489 insulin$^+$-cells scored) (**e**) and inversely, 93% of the YFP$^+$ cells are insulin$^+$ (**f**) (control: $n = 3$; absent YFP$^+$-cells in all control conditions; DT: $n = 3$, 478 YFP$^+$-cells scored). **g**, Experimental design to block Ngn3 upregulation in β-cell-ablated prepubescent mice by administrating DOX to mice bearing five mutant alleles: *Ngn3-tTA*$^{+/+}$; *TRE-Ngn3*$^{+/+}$; *RIP-DTR*. In these mice the *Ngn3* coding region is replaced by a DOX-sensitive transactivator gene (tTA); the endocrine pancreas develops normally because Ngn3 expression is allowed in the absence of DOX by the binding of tTA to the promoter of the *TRE-Ngn3* transgene. Pups were given DT at 2 weeks of age and then DOX 2 weeks later, to block Ngn3 upregulation. They were euthanized when Ngn3 peaks after ablation (2-month-old). **h**, Islets from non-ablated (no DT) and ablated (DT) mice, exposed (Ngn3 inhibition) or not (normal Ngn3 expression) to DOX treatment from 4 weeks of age. β-Cell regeneration is efficient in absence of DOX (as previously shown), but decreases after Ngn3 blockade, resulting in the appearance of glucagon/insulin bihormonal cells. **i**, Sharply decreased regeneration by blocking Ngn3 expression in DOX-treated mice reveals the requirement of Ngn3 for efficient β-cell regeneration in pups. DT: $n = 266$ islets scored, 3 mice; DT+DOX: $n = 167$, 4 mice. Welch's test (inter-islet $P < 0.0001$; inter-animal $P = 0.0352$), Mann–Whitney ($P < 0.0001$). **j**, Glucagon$^+$/insulin$^+$ bihormonal cells appear in DOX-treated β-cell-ablated pups (Ngn3 inhibition), suggesting a switch to an 'adult-like', less efficient, mechanism of regeneration. Control+DOX: $n = 3$, 9,233 insulin$^+$-cells scored; DT: $n = 3$, 1,385 insulin$^+$-cells scored; DT+DOX: $n = 4$, 141 insulin$^+$-cells scored. Welch's test ($P = 0.0081$), ANOVA ($P < 0.0001$). **k**, Combined double lineage tracing of δ-cells (Tomato$^+$) and Ngn3-expressing cells (YFP$^+$) shows by immunofluorescence that nearly all insulin$^+$ cells express both reporters, but no Sst (arrows). Sst$^+$ cells (arrowheads) are YFP- and insulin-negative. Scale bars, 20 μm. Error bars show s.d.

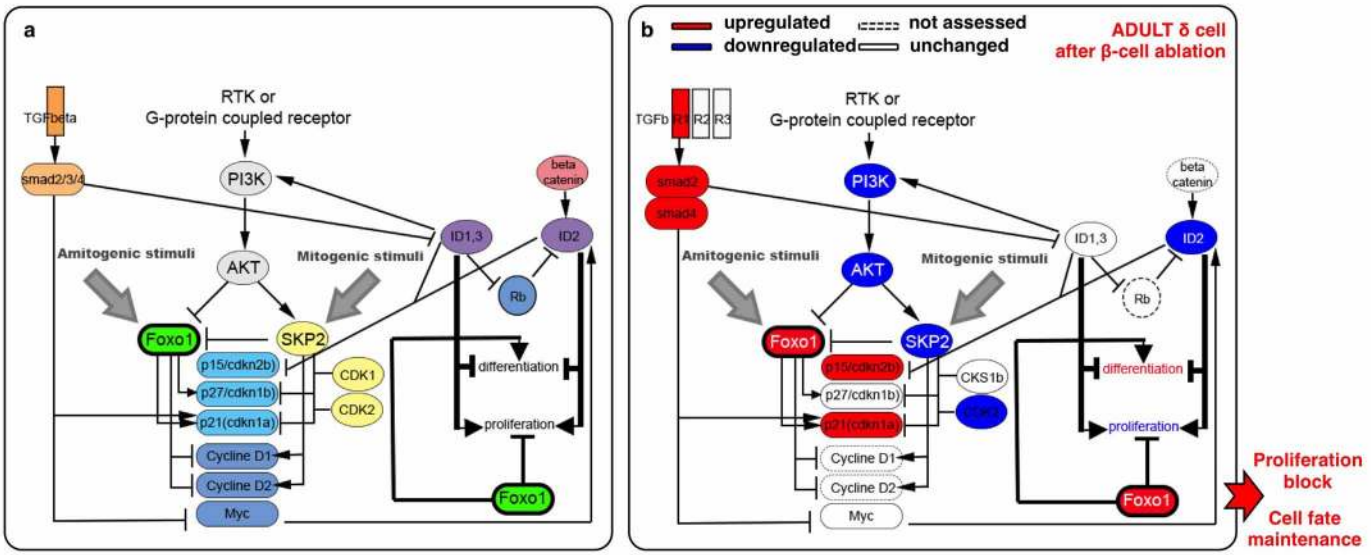

Extended Data Figure 9 | FoxO1 regulatory network. **a**, Cartoon depicting the FoxO1 network involved in the regulation of cell cycle progression and cellular senescence: FoxO1 arrests the cell cycle by repressing activators (cyclin D1, cyclin D2) and inducing inhibitors (Cdkn1a, Cdkn1b, Cdkn2b, Cdkn1c) (PMID: 10102273; PMID: 17873901). Cdkn1a and Cdkn2b activation, a sign of cellular senescence (PMID: 17667954), is regulated by FoxO1 through direct interaction with Skp2 protein. In turn, Skp2 blocks FoxO1 and, together with CKS1b, CDK1 and CDK2, triggers the direct degradation of Cdkn1a and Cdkn1b, thus promoting proliferation (PMID: 15668399). FoxO proteins are inhibited mainly through PI3K/AKT-mediated phosphorylation (PMID: 10102273; PMID: 12621150; PMID: 21708191; PMID: 10217147; PMID: 17604717]: PDK1, the master kinase of the pathway, stimulates cell proliferation and survival by directly activating AKT, which phosphorylates (inhibits) the FoxOs (PMID: 10698680; PMID: 19635472). The PI3K/AKT/FoxO1 circuit requires active TGF-β/SMAD signalling (PMID: 24238962; PMID: 15084259) in order to co-regulate Cdkn1a-dependent cell senescence. Active TGF-β signalling downregulates the BMP pathway downstream effectors ID1 and ID2, known to promote dedifferentiation and proliferation during embryogenesis and cancer progression, probably through Cdkn2b regulation (PMID: 11840321; PMID: 16034366). **b**, β-cell ablation in adults triggers FoxO1 upregulation and the subsequent cell cycle arrest in δ-cells.

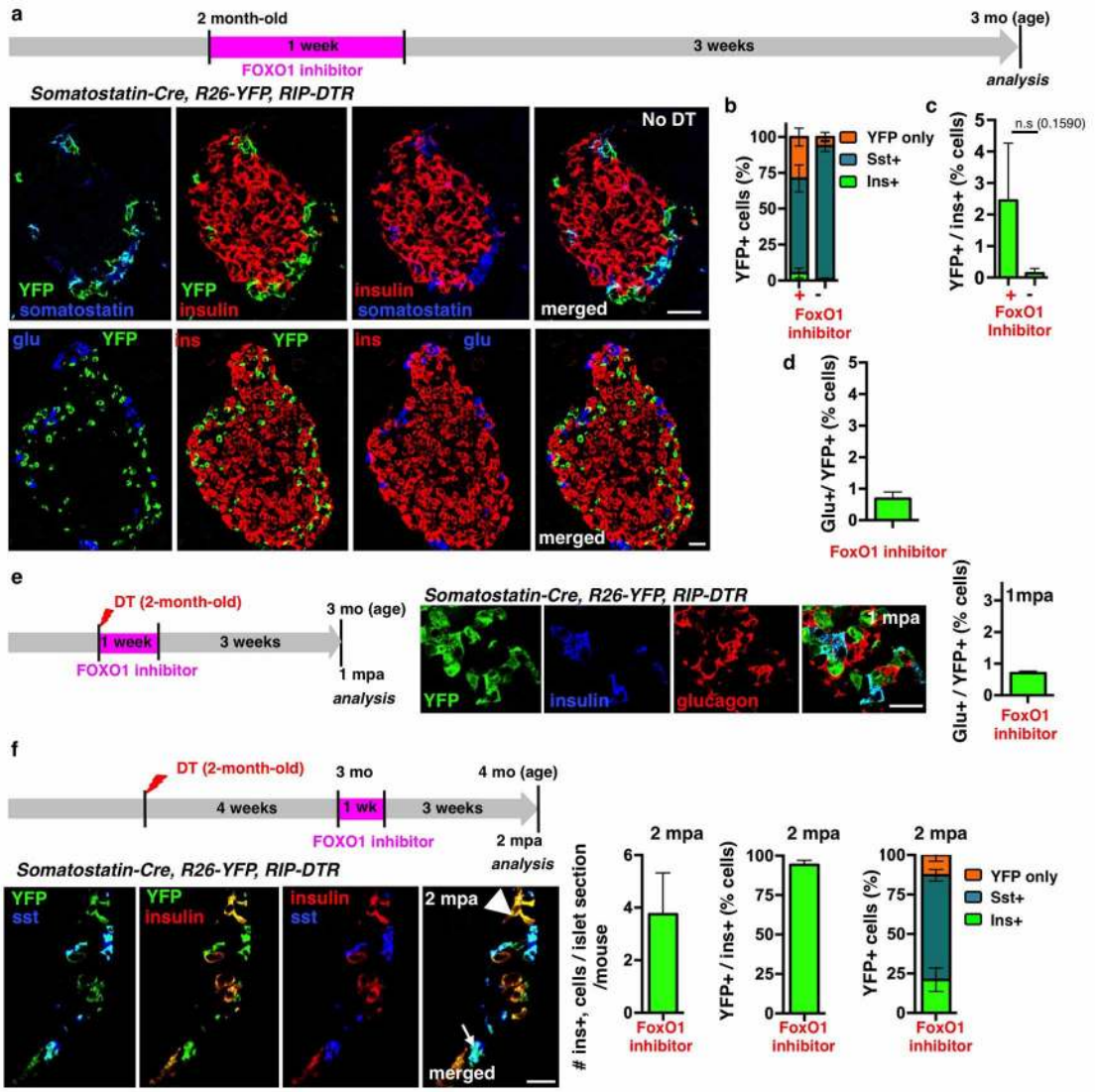

Extended Data Figure 10 | δ-cell dedifferentiation in adult mice upon transient FoxO1 inhibition. **a**–**d**, The 1 week FoxO1 inhibition with the compound AS1842856 in control unablated adult mice (**a**) results in dedifferentiation of one-fourth of the δ-cell population (**b**; Supplementary Table 30) (treated: $n = 3$, 1,347 YFP^+-cells scored; untreated: $n = 4$, 1,224 YFP^+-cells scored; error bars show s.d.), without leading to insulin (**c**; Supplementary Table 31) (treated: $n = 3$, 3,249 $insulin^+$-cells scored; untreated: $n = 4$, 9,562 $insulin^+$-cells scored; error bars show s.d.; Welch's test ($P = 0.1590$)) or glucagon (**d**; Supplementary Table 32) (treated: $n = 2$, 728 YFP^+-cells scored; error bar show s.e.m.) expression. **e**, One month following FoxO1 transient inhibition in β-cell-ablated adults, dedifferentiated δ-cells do not express glucagon (Supplementary Table 36) (treated: $n = 2,986$ YFP^+-cells scored; error bars show s.e.m.). **f**, Transient FoxO1 inhibition a long time (1 month) after β-cell ablation also leads to the appearance of lineage-traced dedifferentiated δ-cells that express insulin (Supplementary Tables 37–39) (treated: $n = 3$, 71 islets scored; 300 $insulin^+$-cells scored; 1,216 YFP^+-cells scored; error bars show s.d.). Scale bars, 20 μm.